

Concerning the Kinetics of Polypeptide Synthesis on Polyribosomes

CAROLYN T. MACDONALD* and JULIAN H. GIBBS, *Department of
Chemistry, Brown University, Providence, Rhode Island, 02912*

Synopsis

The kinetics of biosynthesis of polypeptides on polyribosomes is analyzed in accordance with a simple mathematical model. Each ribosome is assumed to block L adjacent (m-RNA) template sites but to move a distance of one, and only one, template site (nucleotide triplet) upon the addition of each monomer unit to the growing polypeptide chain bound to it. Solutions are sought for the probability, $n_j(t)$, that a template possesses, at time t , a polypeptide chain that has reached degree of polymerization j .

Several classes of steady-state solutions are obtained via machine computation. These correspond to various choices of relative rates of initiation, polymerization along templates, and termination (release of completed chains from templates).

Experimental data available from radioactive pulse labeling experiments are discussed. The data obtained by Dintzis, and by Winslow and Ingram, in studies of the synthesis of the α chain of rabbit hemoglobin and human hemoglobin, respectively, are consistent with steady-state solutions obtained from the current theoretical calculations when the rates of initiation and termination are of comparable magnitude and rate-determining. In this case, a (relatively) small number of chains are polymerized at a (relatively) fast rate each near the beginning of the template, and there exists a transition to a situation near the end of the template in which a (relatively) large number of chains are polymerized at a (relatively) slow rate each. For this solution the situation near the end of the template is entirely analogous to a traffic jam in automobile traffic.

Introduction

The biosynthesis of a polypeptide chain is known to proceed, through the agency of a ribosome, sequentially along a messenger RNA (m-RNA) template, via the addition of monomers only. Each amino acid residue is initially incorporated at the growing chain end (polymerization center) in the form of its transfer RNA (t-RNA) derivative, the t-RNA being eliminated upon the incorporation of the succeeding amino-acyl-t-RNA. Since each growing polypeptide chain is directly bound to the m-RNA only through the t-RNA at its growing end, it is possible for more than one polypeptide chain of a given type to grow on the same template at the same time. However, the requirement that each polymerization step be accompanied by a motion of the reacting polymerization center through a distance of one template site in a definite direction along the m-RNA

* Present address: Department of Chemistry, Moorhead State College, Moorhead, Minnesota, 56560.

template implies the possibility, in such multiple synthesis, of the growth of one polypeptide chain being impeded by the presence of another preceding it on the template.

This article is the third of a series dealing with the kinetics of template directed polymerizations catalyzed by *exo*-enzymes. In Part I, Pipkin and Gibbs¹ discussed a case in which only one new polymer chain may grow on a given template at a given time. In Part II, MacDonald, Gibbs, and Pipkin² began the discussion of a theoretical model for cases, such as that of polypeptide biosynthesis, in which there may be simultaneous but mutually interfering syntheses of several or many new chains on a common template molecule. This article extends the treatment of Part II to the point of meaningful contact between theory and experiment in the case of polypeptide biosynthesis.

Since the association of peptidyl t-RNA with m-RNA appears to be unstable in the absence of ribosomes, and since the coding registration of each peptidyl t-RNA with m-RNA must be maintained throughout the course of polypeptide synthesis, it is reasonable to assume that no component of a given complex, peptidyl-t-RNA-ribosome-m-RNA, dissociates from the others of the same complex during the period between its successive polymerization events. The polymerization center should thus be viewed as a complex consisting of a growing chain end and the corresponding ribosome. Although the growing chain end probably occupies, through its terminal t-RNA, only one template site (nucleotide triplet or codon) at a time, the corresponding ribosome is quite large and can block more than one site. The total number of sites blocked by a polymerization center will be designated as L .

The considerations of the foregoing paragraphs lead to the concept that the process of polypeptide synthesis is analogous to the biased diffusion, on a single one-dimensional lattice, of several nonoverlapping segments, each segment occupying L adjacent lattice sites but moving in steps of single lattice spacings. Thus, in order to treat the kinetics of polypeptide synthesis theoretically, we consider an ensemble of systems, with each system consisting of a lattice of K sites plus the segments diffusing on it. The K sites of a lattice are numbered consecutively from beginning to end. Each segment in the ensemble is of length L . Each lattice site has $L + 1$ states available to it, L modes of occupation and one mode of emptiness. A lattice site j is designated as being in state 0 if it is empty and in state s (where $s = 1, 2, \dots, L$) if it is the s th site covered by one segment, i.e., if a segment occupies sites $j - s + 1, \dots, j - s + L$. For $s = 0, 1, \dots, L$, let $n_j^{(s)}(t)$ be the fraction of systems in the ensemble with site j in state s at time t , and let $q_j^{(s)}(t)$ be the flux of occupancy of type s from site j to site $j + 1$ at time t . Conservation requires that

$$dn_j^{(s)}(t)/dt = q_{j-1}^{(s)}(t) - q_j^{(s)}(t) \quad (1)$$

In eq. (9) of Part II,² an expression is given for $q_j^{(L)}(t)$ [called $q_j(t)$ in Part II] in terms of the $n_j^{(L)}(t)$. Here, however, we wish to allow more

specifically, if only formally and temporarily, for the possibility that the effective "rate constants" (written simply as k_f and k_b in Part II) associated with the forward and backward contributions to the $q_j^{(L)}(t)$ may depend upon j and t (see below). More appropriately, we wish to write them as functions of $j - L + m$ (and t), if the polymerization site (site to which the peptidyl t-RNA is bonded) is the m th site covered by the ribosome. Accordingly, we assign them superscripts $[j - L + m]$ and write eq. (9) of Part II as

$$q_j^{(L)}(t) = k_f^{[j-L+m]}(t) \frac{n_j^{(L)}(t) \left[1 - \sum_{s=1}^L n_{j+s}^{(L)}(t) \right]}{1 - \sum_{s=1}^L n_{j+s}^{(L)}(t) + n_{j+L}^{(L)}(t)} - k_b^{[j-L+m]}(t) \frac{n_{j+1}^{(L)}(t) \left[1 - \sum_{s=1}^L n_{j-L+s}^{(L)}(t) \right]}{1 - \sum_{s=1}^L n_{j-L+s}^{(L)}(t) + n_{j-L+1}^{(L)}(t)} \quad (2)$$

Necessary in the derivation of eq. (2) are the assumption that the motions of the ribosomes are independent except for the no-overlap restriction ("hard segment" model) and the related assumption that the conditional probability that lattice site $j + 1$ is in state 0, given that j is in stage L , is the same as the conditional probability that site $j + 1$ is in state 0, given that j is in state 0.

The appropriate amino acyl t-RNA concentration, i.e., the one upon which depends the rate of the reaction transferring mode of occupancy L from site j to site $j + 1$, is included as a factor in $k_f^{[j-L+m]}(t)$. Similarly, $k_b^{[j-L+m]}(t)$ contains as factors the appropriate "uncharged" t-RNA and water concentrations. Since the amino acyl t-RNA and uncharged t-RNA may not be present in large excess, and since they may not always be maintained in the constant concentrations of a steady state, even *in vivo*, they may be time dependent in some biological situations. Thus they are better described as "specific rates" than as "effective rate constants".

Although we are here deferring restrictive assumptions concerning the specific rates $k_f^{[j-L+m]}(t)$ and $k_b^{[j-L+m]}(t)$ as long as possible, we will eventually need to complete the formulation of our problem with some postulate concerning their nature. In the absence of any specific information concerning the values of these specific rates for the individual polymerization steps, it seems appropriate to treat the simplest case, namely, the one in which they are all taken as equal though different from the specific rates of initiation and termination. In Part II this assumption was made, and two special cases were considered: uniform-density solutions, for which $n_j^{(L)}(t) = n$ (and $k_f^{[j-L+m]}(t) = k_f$, $k_b^{[j-L+m]}(t) = k_b$), and steady-state solutions, for which $dn_j^{(L)}(t)/dt = 0$ (and $k_f^{[j-L+m]}(t) = k_f$, $k_b^{[j-L+m]}(t) = k_b$). Analytical solutions were found for all L in the

uniform-density case and for only $L = 1$ in the steady-state case. This article will extend the treatment of the steady-state case to $L > 1$. The solutions obtained are compared with available experimental results.

Boundary Conditions

The flux equation, eq. (2), is written in terms of the $n_j^{(L)}(t)$, where $n_j^{(L)}(t)$ is the probability that the complex of growing chain end plus ribosome blocks the sites $j - L + 1, \dots, j$. The actual site for polymerization is the site which the chain end occupies. In general it is one of the central sites blocked by the ribosome and has been designated as the m th site ($1 \leq m \leq L$), with m fixed for a given system. Then $n_{j-m+L}^{(L)}(t)$ is the probability that a template has a polymer that has grown to degree of polymerization j . It is more convenient to consider instead the variable $n_j^{(m)}(t)$, which is also the probability that a template has a polymer of degree j , or equivalently, the probability that the entire growing center blocks the sites $j - m + 1, \dots, j - m + L$.

Since

$$n_j^{(L)}(t) = n_{j-L+m}^{(m)}(t)$$

and

$$q_j^{(L)}(t) = q_{j-L+m}^{(m)}(t),$$

a simple transition of variables in eq. (2) gives an equation in $q_j^{(m)}(t)$ and $n_j^{(m)}(t)$ which is identical in form to eq. (2), but with the superscript (m) substituted for the superscript (L) . We now drop the superscript (m) and let

$$n_j^{(m)}(t) = n_j(t)$$

and

$$q_j^{(m)}(t) = q_j(t)$$

In this simplified notation, the flux equation, eq. (2), becomes

$$q_j(t) = k_f^{[j]}(t) \frac{n_j(t) \left[1 - \sum_{s=1}^L n_{j+s}(t) \right]}{1 - \sum_{s=1}^L n_{j+s}(t) + n_{j+L}(t)} - k_b^{[j]}(t) \frac{n_{j+1}(t) \left[1 - \sum_{s=1}^L n_{j-L+s}(t) \right]}{1 - \sum_{s=1}^L n_{j-L+s}(t) + n_{j-L+1}(t)} \quad (3)$$

In eq. (3), $n_j(t)$ is the probability that the template has a polymer of degree j , and $q_j(t)$ is the flux of the growing chain end.

Physically, a degree of polymerization of 1 to K is possible, and the variables n_1, \dots, n_K have a definite physical meaning. The flux equation, eq. (3), holds only in the interior of the lattice, for $L \leq j \leq K - L$. At the ends, it must be modified to incorporate the special boundary conditions.

In order to determine the appropriate boundary conditions, it is necessary to consider the mechanism by which the growing center attaches and detaches from the template.

Initiation of polymerization begins when a ribosome (enzyme) attaches to the template and begins polymerization by moving along the template. It is assumed that the ribosome attaches in a position such that site 1 is in the m th mode of occupancy, i.e., the ribosome attaches such that the amino acyl t-RNA beginning the chain occupies lattice site 1. In order for this to occur, sites $1, \dots, L - m + 1$ must be empty simultaneously to allow room for the large ribosome to attach to the template. Similarly, if the initial polymerization step reverses, it is assumed that the monomer and ribosome are detached simultaneously from the template, vacating sites $1, \dots, L - m + 1$. This postulated mechanism of attachment and detachment implies that sites $1, \dots, L - m$ will be empty if and only if site $L - m + 1$ is empty. Thus the probability of sites $1, \dots, L - m + 1$ simultaneously being empty is equal to

$$n_{L-m+1}^{(0)}(t) = 1 - \sum_{s=1}^L n_s(t)$$

Thus, for the initiation step, there should be a forward flux on to site 1 of the lattice proportional to $1 - \sum_{s=1}^L n_s(t)$ and a backward flux off the lattice proportional to the probability that site 1 is in state m . The specific rates for these steps do not need to be the same as any of the forward and backward specific rates in the interior, $k_f^{(j)}(t)$ and $k_b^{(j)}(t)$. The boundary conditions described for the initiation step can be written as

$$q_0(t) = k_f^{(0)}(t) \left[1 - \sum_{s=1}^L n_s(t) \right] - k_b^{(0)}(t) n_1(t)$$

For $j = 1, \dots, L - 1$, the forward flux takes the same form as the forward flux in the lattice interior. However, for $L > 1$, the method of detachment from the lattice gives a different form for the backward flux. For $j = 1, \dots, L - 1$, the backward motion of a chain from polymerization degree $j + 1$ to degree j can not be blocked as there can be no additional growing center less far along on the template. Thus, the backward flux takes the simple form $k_b^{(j)} n_{j+1}(t)$. The boundary conditions are

$$q_j(t) = k_f^{(j)}(t) \frac{n_j(t) \left[1 - \sum_{s=1}^L n_{j+s}(t) \right]}{1 - \sum_{s=1}^L n_{j+s}(t) + n_{j+L}(t)} - k_b^{(j)}(t) n_{j+1}(t)$$

$$1 \leq j \leq L - 1$$

Release from the template of the completed polymer occurs when the growing chain has reached degree K . It is assumed that the completed chain and ribosome, which have been blocking sites $K - m + 1, \dots, K$, are released simultaneously from the template. Thus, when a growing

chain reaches polymerization of degree j , for $K - L + 1 \leq j \leq K - 1$, its forward motion can no longer be blocked as there can be no additional growing center further along on the template. The forward flux is then $k_f n_j(t)$. For $j = K - L + 1, \dots, K - 1$, the backward flux takes the same form as the backward flux in the interior. Thus, the boundary conditions are

$$q_j(t) = k_f^{[j]}(t) n_j(t) - k_b^{[j]}(t) \frac{n_{j+1}(t) \left[1 - \sum_{s=1}^L n_{j-L+s}(t) \right]}{1 - \sum_{s=1}^L n_{j-L+s}(t) + n_{j-L+1}(t)}$$

$$K - L + 1 \leq j \leq K - 1$$

For the termination step of release from the template of a completed chain, the forward flux is proportional to the probability that site K is in state m . For flux of the chain back on to site K , sites $K - m + 1, \dots, K$ must be simultaneously empty in order to allow room for the ribosome to attach to the template with site K in occupation mode m . The probability of sites $K - m + 1, \dots, K$ being simultaneously empty is equal to

$$n_{K-m+1}^{(0)}(t) = 1 - \sum_{s=1}^L n_{K-L+s}(t)$$

The rate constants for these steps do not need to be the same as the interior rate constants or the rate constants for the initiation step. The boundary condition for termination can be written

$$q_K(t) = k_f^{[K]}(t) n_K(t) - k_b^{[K]}(t) \left[1 - \sum_{s=1}^L n_{K-L+s}(t) \right]$$

In summary, the flux equations can be written as

$$q_0(t) = k_f^{[0]}(t) \left[1 - \sum_{s=1}^L n_s(t) \right] - k_b^{[0]}(t) n_1(t) \quad (4a)$$

$$q_j(t) = k_f^{[j]}(t) \frac{n_j(t) \left[1 - \sum_{s=1}^L n_{j+s}(t) \right]}{1 - \sum_{s=1}^L n_{j+s}(t) + n_{j+L}(t)} - k_b^{[j]}(t) n_{j+1}(t)$$

$$1 \leq j \leq L - 1 \quad (4b)$$

$$q_j(t) = k_f^{[j]}(t) \frac{n_j(t) \left[1 - \sum_{s=1}^L n_{j+s}(t) \right]}{1 - \sum_{s=1}^L n_{j+s}(t) + n_{j+L}(t)}$$

$$- k_b^{[j]}(t) \frac{n_{j+1}(t) \left[1 - \sum_{s=1}^L n_{j-L+s}(t) \right]}{1 - \sum_{s=1}^L n_{j-L+s}(t) + n_{j-L+1}(t)} \quad L \leq j \leq K - L \quad (4c)$$

$$q_j(t) = k_f^{[j]}(t) n_j(t) - k_b^{[j]}(t) \frac{n_{j+1}(t) \left[1 - \sum_{s=1}^L n_{j-L+s}(t) \right]}{1 - \sum_{s=1}^L n_{j-L+s}(t) + n_{j-L+1}(t)} \quad K - L + 1 \leq j \leq K - 1 \quad (4d)$$

$$q_K(t) = k_f^{[K]}(t) n_K(t) - k_b^{[K]}(t) \left[1 - \sum_{s=1}^L n_{K-L+s}(t) \right] \quad (4e)$$

In the remaining sections of this paper, we restrict our attention to specific rates which are independent of t , and, for $1 \leq j \leq K - 1$, independent of j :

$$\begin{aligned} k_f^{[0]}(t) &= k_f^{[0]} \\ k_f^{[j]}(t) &= k_f \\ k_b^{[j]}(t) &= k_b \\ k_f^{[K]}(t) &= k_f^{[K]} \quad 1 \leq j \leq K - 1 \end{aligned} \quad (5)$$

We now examine two special sets of solutions of eq. (4), the uniform density solutions, for which $n_j(t) = n(t)$, and the steady-state solutions, for which $dn_j(t)/dt = 0$.

Uniform Density Solutions

If $n_j(t) = n(t)$ for $L + 1 \leq j \leq K - L$, eq. (4c) gives $q_j(t) = q(t)$ for $2L \leq j \leq K - 2L$. Substitution of this into eq. (1) gives $n_j(t) = n(t) = n$ for $2L + 1 \leq j \leq K - 2L$, and hence $n_j(t) = n$ for $L + 1 \leq j \leq K - L$. The interior flux equation, eq. (4c) is then

$$q_j(t) = q = (k_f - k_b) n(1 - Ln)/[1 - (L - 1)n] \quad L \leq j \leq K - L \quad (6)$$

By the term uniform-density flux, we will henceforth mean the interior flux, q , as given by eq. (6).

The maximum interior flux, q_{\max} ,

$$q_{\max} = (k_f - k_b)/(1 + \sqrt{L})^2 \quad (7)$$

occurs when

$$n_j \equiv n_{\max} = 1/\sqrt{L}(1 + \sqrt{L}) \quad (8)$$

Given a q such that $q < q_{\max}$, there are two solutions for n_j that give the same interior flux q . Solution of the quadratic equation, eq. (6), gives a low-density solution, $n_j \equiv n < n_{\max}$, and a high-density solution, $n_j \equiv (1 - Ln)/L[1 - (L - 1)n]$.

Steady-State Solutions

If $dn_j(t)/dt = 0$, then eq. (1) gives $q_j(t) = q(t)$ for all j and eq. (4) gives $q(t) = q$ for all j . The flux equation, eq. (4c), in this case is

$$q = k_f \frac{n_j \left(1 - \sum_{s=1}^L n_{j+s}\right)}{1 - \sum_{s=1}^L n_{j+s} + n_{j+L}} - k_b \frac{n_{j+1} \left(1 - \sum_{s=1}^L n_{j-L+s}\right)}{1 - \sum_{s=1}^L n_{j-L+s} + n_{j-L+1}} \quad (9)$$

Equation (6) is preserved as the definition of n in the steady-state case. In the uniform-density case, n represented an actual probability and was required to be real, $0 \leq n \leq 1/L$. These restrictions are not made in the steady-state case. When $q < q_{\max}$, the solution of the quadratic equation, eq. (6), for n gives n real, $0 \leq n \leq 1/L$, $n \neq 1/\sqrt{L}(1 + \sqrt{L})$. For $q = q_{\max}$, $n = 1/\sqrt{L}(1 + \sqrt{L})$. When $q > q_{\max}$, i.e., when the steady-state flux is larger than the maximum flux allowed for the uniform density case, n is a complex number.

The steady-state solutions for the occupation density n_j as a function of j for $L = 1$ were discussed in detail in Part II. Analytic solutions to the flux equation were obtained and graphed. For $L > 1$, analytic solutions have not been found. However, by analogy with the case $L = 1$, an examination of the flux equation and the physical conditions yields a number of hypotheses concerning the nature of the solutions for $L > 1$. The hypotheses can then be tested by programming the equations on a computer. The results are discussed in detail by MacDonald.³ The treatment was restricted to the special case with $k_b = 0$. In general, the hypotheses were found to be correct.

For all L , when $0 < q < q_{\max}$, there are three classes of solutions for n_j as a function of j , low-density solutions, high-density solutions, and solutions that are a composite of the previous two classes, being low-density for small j and exhibiting a transition to high-density for large j .

The low-density solutions are nearly uniform except for very large j . The value assumed in the nearly uniform region is the smaller uniform-density root corresponding to the given flux, which is $\min\{n, (1 - Ln)/[1 - (L - 1)n]\}$, where $q = k_f n(1 - Ln)/[1 - (L - 1)n]$. The low-density solutions occur when initiation is the rate-determining step. The two types of low-density solutions are shown in Figures 1A and 2A for $L = 2$.

The high-density solutions for $L = 1$ only are nearly uniform except for very small j . The value assumed in the nearly uniform region is the larger uniform-density root corresponding to the given flux. The high-density solutions occur when release of the completed chain from the template is the rate-determining step and correspond to a pile-up of growing chains at the end of the template. In the case $L > 1$, however, there is an additional effect of "blocking" on the nature of the high-density solutions. Since the minimum distance allowed between two growing chains

is L , high density occurs at the sites $K - pL$, with p an integer. The $L - 1$ sites between two adjacent high-density sites are accordingly at a lower density, assuming a value such that the average of the occupation densities over one "period", consisting of $L - 1$ low-density sites and the adjacent high-density site, is approximately equal to the larger uniform-density root corresponding to the given flux, i.e., $\max \{n, (1 - Ln)/(1 - (L - 1)n)\}$. The high-density solutions can thus be viewed as oscillating with "period" L about the larger uniform-density root. The two types of high-density solutions are shown in Figures 3A and 4A for $L = 2$.

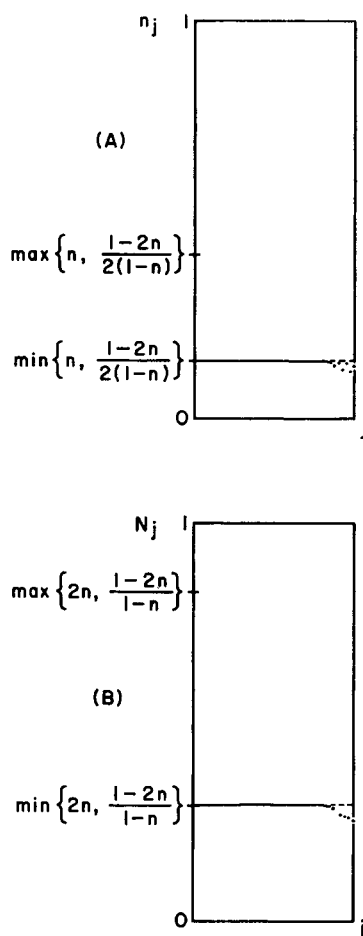


Fig. 1. An example of one of the two types of low-density solutions of the flux equation for $L = 2$ with $k_b = 0$ and $q < q_{\max} = k_f/(1 + \sqrt{2})^2$: (A) chain end occupation density, n_j , as a function of j ; (B) total occupation density, N_j , as a function of j , with $m = 2$. $N_j = n_j + n_{j+1}$. $q = k_f n(1 - 2n)/(1 - n) = k_f n_j(1 - n_{j+1} - n_{j+2})/(1 - n_{j+1})$. The low-density solutions occur when initiation is the rate-determining step. The other type of low-density solution is shown in Figure 2.

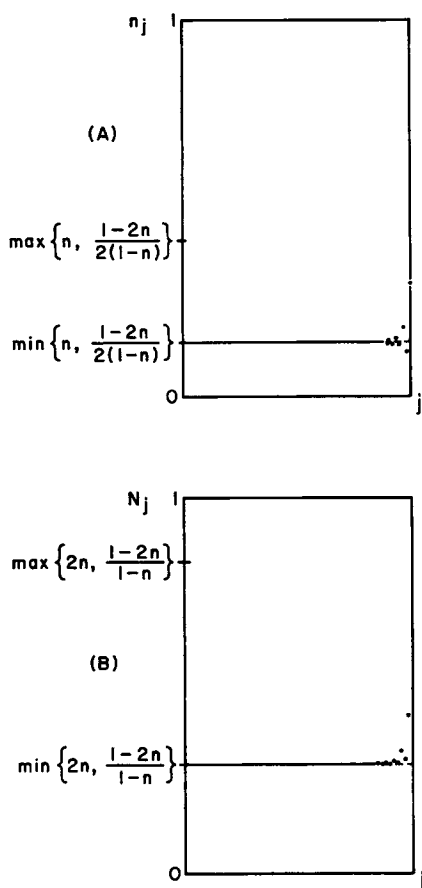


Fig. 2. An example of the second of two types of low-density solutions for $L = 2$ with $k_b = 0$ and $q < q_{\max}$.

The solutions of the third class are nearly uniform to the smaller uniform-density root for small j , with a transition to a high-density region with oscillation about the larger uniform-density root for large j . This class of solutions has particular relevance to the experimental data examined below. This type of solution is illustrated in Figure 5A for $L = 2$ and in Figure 6A for $L = 27$.

When $q = q_{\max}$, the same results hold, except that in this case, the two uniform-density roots are equal, with the value $1/\sqrt{L}(1 + \sqrt{L})$.

For $q > q_{\max}$, i.e., when the steady-state flux is larger than the maximum flux allowed for the uniform-density case, the solutions will approach the uniform solution $1/\sqrt{L}(1 + \sqrt{L})$, except for very small j and very large j , provided the lattice is of proper length. An example of this type of solution is shown in Figure 7A for $L = 2$.

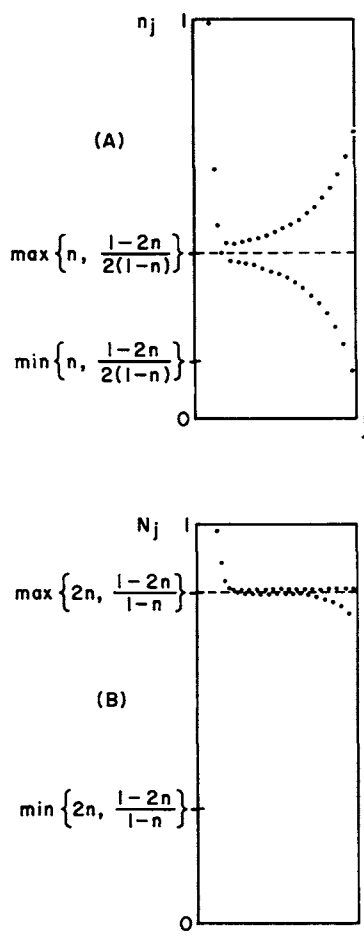


Fig. 3. An example of one of the two types of high-density solutions for $L = 2$ with $k_b = 0$ and $q < q_{\max}$. The high-density solutions occur when release of the completed chain from the template is the rate-determining step. The other type is shown in Figure 4.

In order to remove part of the oscillatory nature of the high-density solutions, we consider a new variable N_j , defined as the total probability of occupancy of site j by any of the L modes of occupancy. Clearly,

$$N_j = 1 - n_j^{(0)} = \sum_{s=1}^L n_{j+s-m-L-1} \quad (10)$$

At first it seems that N_j might be the closest analog to n_j in the case $L = 1$, being nearly uniform in a high-density region. However, examination of the flux equation for the non-saturated steady-state case indicates that N_j is uniform if and only if n_j is uniform. Thus, when n_j oscillates

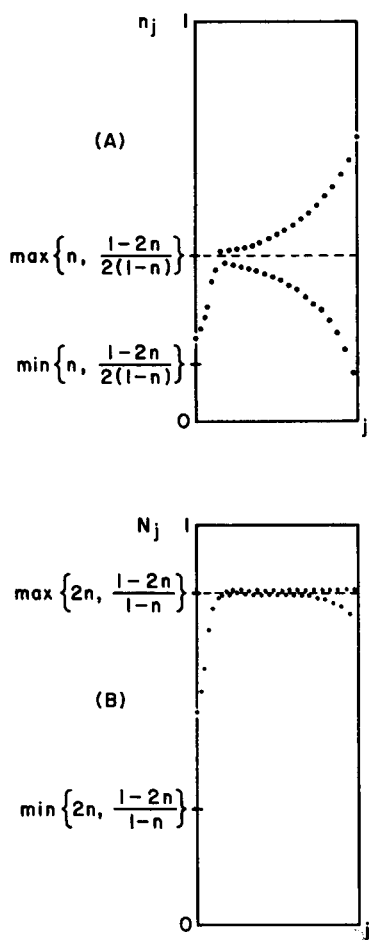


Fig. 4. An example of the second of two types of high-density solutions for $L = 2$ with $k_b = 0$ and $q < q_{\max}$.

N_j also oscillates, although with a lesser relative amplitude than n_j . The graphs for N_j corresponding to the solutions for n_j in the various cases are illustrated in Figures 1B–7B. One difficulty in dealing with N_j is that the flux equation can not be written in terms of the N_j only.

The appropriate solution curves are determined by the boundary conditions given in eq. (4). In the special case $k_b^{[0]} = k_b^{[K]} = 0$ and $k_b = 0$, hypotheses concerning the nature of the solutions were postulated and tested.³

For $k_f^{[0]} < k_f^{[K]}$ and $k_f^{[0]} < k_f/(1 + \sqrt{L})$, the solution is a low-density solution and is nearly uniform to the value $k_f^{[0]}/[k_f + (L - 1)k_f^{[0]}]$ except for large j .

For $k_f^{[K]} < k_f^{[0]}$ and $k_f^{[K]} < k_f/(1 + \sqrt{L})$, the solution is a high-density solution and oscillates about $(k_f - k_f^{[K]})/k_f L$ with "period" L .

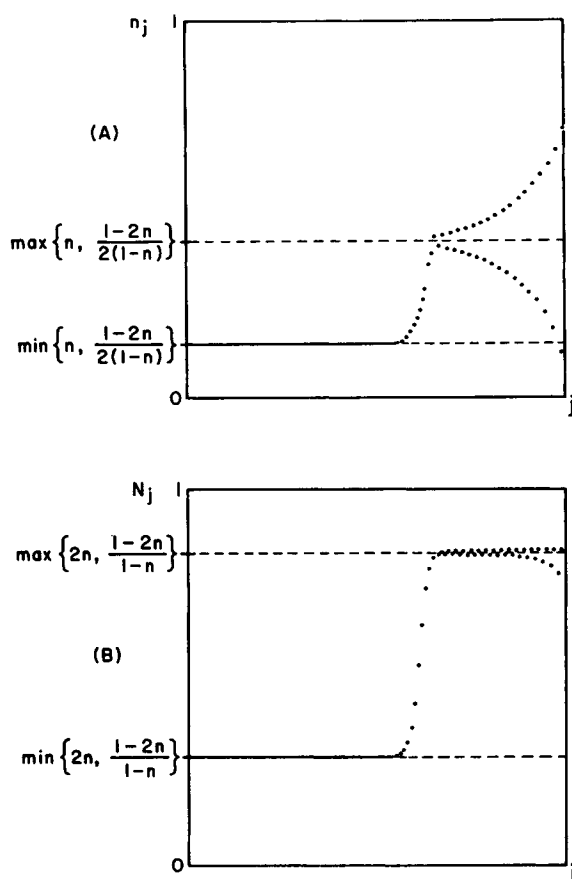


Fig. 5. An example of the class of solutions with a transition from low density to high density for $L = 2$ with $k_b = 0$ and $q < q_{\max}$. These solutions occur when initiation and release from the template are of comparable magnitude and are rate-determining.

When $k_f^{[0]}$ and $k_f^{[K]}$ are nearly equal and also less than $k_f/(1 + \sqrt{L})$, the solution is nearly uniform to $k_f^{[0]}/[k_f + (L - 1)k_f^{[0]}]$ for small j and oscillates with period L about $(k_f - k_f^{[K]})/k_f L$ for large j , with a transition between the low-density and high-density solutions in the interior.

If $k_f^{[0]} > k_f/(1 + \sqrt{L})$ and $k_f^{[K]} > k_f/(1 + \sqrt{L})$, the solution is nearly uniform to $1/\sqrt{L}(1 + \sqrt{L})$ except for very small j and for very large j .

In each case the flux is given by

$$q = k_f \left[\frac{m(1 - m)}{1 + (L - 1)m} \right] \quad (10a)$$

with

$$m = \min\{k_f^{[0]}/k_f, k_f^{[K]}/k_f, 1/(1 + \sqrt{L})\} \quad (10b)$$

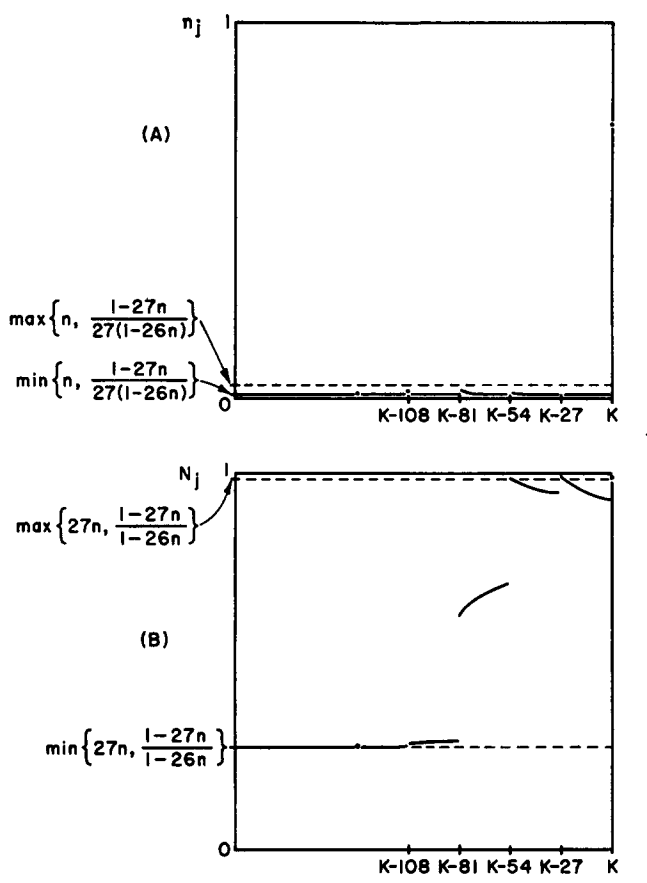


Fig. 6. An example of one of the three main classes of solutions of the flux equation for $L = 27$ with $k_b = 0$ and $q < q_{\max} = k_f/(1 + \sqrt{27})^2$: (A) chain end occupation density, n_j , as a function of j ; (B) total occupation density, N_j , as a function of j , with $m = 1$. $N_j = \sum_{s=1}^{27} n_{j+s-27}$. $q = k_f n(1 - 27n)/(1 - 26n) = k_f n_i(1 - \sum_{s=1}^{27} n_{j+s})/(1 - \sum_{s=1}^{27} n_{j+s} + n_{j+27})$. These solutions for $L = 27$ correspond to those of Figure 5 for $L = 2$.

Comparison with Experiment

The literature on protein synthesis has been examined to determine the conclusions that can be drawn concerning which, if any, of the steady-state solutions may be consistent with the experimental data.

Each lattice (or template) site corresponds to an amino acid residue, or three nucleotides. Since the nucleotides are stacked with a translation of about 3.4 \AA and a ribosome has a diameter of 230 \AA ,⁴ a ribosome would be expected to occupy about 23 consecutive lattice points, giving $L = 23$. Takanami and Zubay,⁵ in studies of poly U as a template for protein

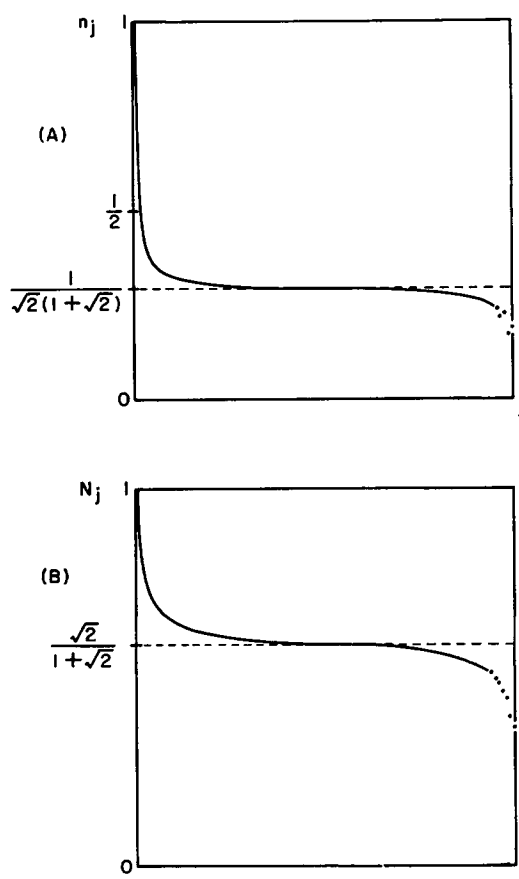


Fig. 7. An example of the class of solutions for $L = 2$ and $k_b = 0$ with $q > q_{\max}$. These solutions occur when polymerization is the rate-determining step.

synthesis, have concluded that a ribosome occupies 27 lattice points. For purposes of the computer calculations in this paper, $L = 27$ was chosen as a representative value.

Slayter et al.,⁴ in addition to determining the size of an individual ribosome, have used electron micrographs to give accurate estimates of the distribution of interribosomal gaps. They found that the ribosomes in a polyribosome were generally separated by gaps of 50–150 Å. The authors pointed out, however, that there was some dependence of the size of the gaps on the method of preparation of the polyribosomes for study. These figures correspond to $\langle N_j \rangle$ in the range 0.61–0.82, with

$$\langle N_j \rangle = \sum_{j=1}^K N_j / K$$

On a hemoglobin chain of 150 amino acid units, this corresponds to a polyribosome containing on the average 3–6 ribosomes, with a maximum

number of 7–8. In a study of rabbit reticulocytes, Warner et al.⁶ found that over 75% of the ribosomes are found in pentamers, with about 10% each in tetramers and hexamers.

For an L of 23, a low uniform-density solution corresponds to $N_j < 0.829$; and for $L = 27$, $N_j < 0.839$. From the range of N_j calculated from the electron micrograph measurements, it would appear that release would probably not be the rate-determining step in such cases (at least not the sole rate-determining step, as this would give a high-density solution for the entire length of the template).

There are a number of experimental results regarding the rate at which a single polypeptide chain is synthesized. By radioactive labeling with ³H-leucine, Dintzis⁷ has concluded that hemoglobin formation in rabbit reticulocytes at 37°C proceeds at a rate averaging about 2 amino acid units per second added to a chain, giving an assembly time of about 1.5 min for each individual polypeptide chain of 150 amino acid units.

Protein synthesis in bacteria occurs at a much faster rate. Goldstein et al.,⁸ in studies on protein synthesis in *E. coli*, found an assembly time for a chain of 400 amino acid units to be 5 sec at 37°C.

In the polyribosome case, care must be taken in interpreting such data. When several chains are being synthesized simultaneously on the same template, it is necessary to distinguish between the rate at which an individual chain grows and the net flux. In the uniform-density case, corresponding to each flux less than the maximum flux there are two different uniform densities that give the same net flux. In the low-density case there are fewer chains being polymerized, and thus each chain must grow at a faster rate in order to give the same net flux as the corresponding high-density case (in which there are more chains growing at one time, but each individual chain grows at a slower rate).

However, the radioactive labeling experiments give direct information about the relative rates of synthesis of an individual chain as it moves along the template and about the steady-state distribution of growing chains on a template.⁹ Some hypothetical relative specific activity curves are shown in Figure 8. These were determined by measurement, after the termination of a labeling pulse, of the radioactivity of the completed chains. Since the label appears along the entire polypeptide chain in the curves shown, these correspond to the case in which the labeling pulse was of longer duration than the time required for an individual chain to be synthesized. As shown in Figure 8, the specific activity curve gives a measure of the steady-state distribution of nascent chain lengths. All completed chains that were of length j_0 or less at the time the pulse was started contribute to the specific activity measured at site j_0 ; i.e., the relative specific activity at site j_0 is directly proportional to $\sum_{j=1}^{j_0} n_j$. The slope of the relative specific activity curve at site j_0 is therefore directly proportional to the occupation density n_{j_0} at site j_0 and inversely proportional to the rate of growth of an individual chain at that site. The hypothetical specific activity curves shown in Figure 8 were chosen

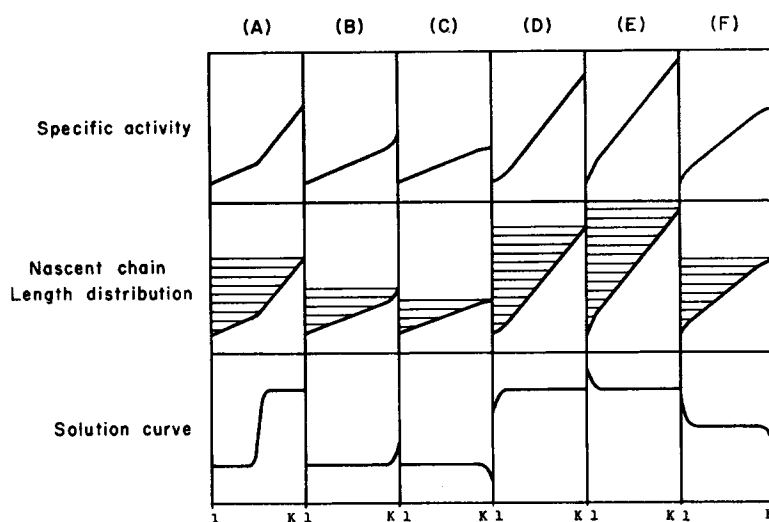


Fig. 8. The hypothetical specific activity curves and nascent chain-length distributions corresponding to the various steady-state occupation density solutions obtained from our model for $L = 1$.

to correspond to the solution curves for the steady-state occupation density obtained from our model with $L = 1$.

In Figure 9 is shown the theoretical specific activity curve that corresponds to the particular steady-state solution for $L = 27$ that is shown in Figure 6. Since only one type of amino acid is labeled in the radioactive labeling experiments, the only points obtained on an experimental specific activity curve are those corresponding to the locations of this amino acid on the chain. A smooth curve is then normally fit to these points. As a result, the staircase detail that corresponds to a high-density region for $L > 1$ would be obscured and would appear instead as a fairly smooth curve of larger slope than the part of the curve corresponding to a low-density region. It is therefore appropriate to consider the simpler shapes of the theoretical curves obtained for $L = 1$.

Studies of the synthesis of rabbit hemoglobin chains^{7,10,11} by pulse labeling with ^3H - and ^{14}C -leucine show that for both α and β chains the plot of the relative specific activity versus position in the chain gives a curve with a small positive slope from the N -terminal position (site 1) up to the 50–100 amino acid position, with a marked increase in slope from there to the C -terminal position (site K). This result was considerably more marked for the α chains. Winslow and Ingram,¹² in similar experiments with human hemoglobin, found essentially the same results. This corresponds to the theoretical curves of Figure 8A and Figure 9. They suggest that a rate change occurs between positions 80 and 100 with a region of rapid growth at the beginning, followed by a region of considerably slower growth at the end. Such a pattern of nonuniform growth, with a region of nearly uniform rapid growth followed by a region of nearly

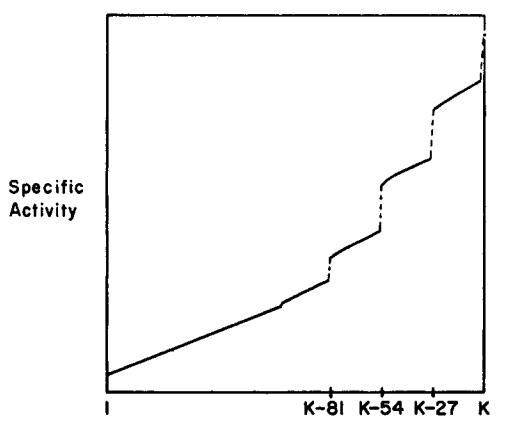


Fig. 9. The hypothetical specific activity curve corresponding to the solution for $L = 27$ shown in Figure 6.

uniform slow growth, is the result of the steady-state case of our model when $k_f^{[0]}$ and $k_f^{[K]}$ are nearly equal and both less than $k_f/(1 + \sqrt{L})$. Here, initiation and release are of comparable magnitude and rate-determining. In this case, there is a region of nearly uniform low-density occupancy (and thus rapid growth) with a transition to a region of high density (with slower growth). This occupation density solution occurs as a natural result of the traffic problem in our model and is not dependent on any assumption of a special rate-controlling polymerization step(s).

Williamson and Schweet,^{13,14} in studies of polymerization in puromycin-treated rabbit reticulocytes, have postulated that the rate-determining step in protein synthesis in both the cell-free system and intact cell is initiation. This would correspond to our nearly uniform low-density solutions, as shown in Figures 8B and 8C.

Theoretically, it should be possible to plot exactly the full specific activity curve for a particular chain by running a series of experiments that label each individual amino acid in turn. However, the shape of a curve, in particular the location of a transition region, is extremely sensitive to the boundary conditions. It is therefore unlikely that an accurate complete curve can be obtainable experimentally *in vivo*. However, adequate information can be obtained from the specific activity curve of a suitably chosen individual amino acid.

This research was supported by grant GM-10906-07 from the United States Public Health Service with assistance from Facilities Grant GP-4825 from the National Science Foundation.

This paper is based in part upon a Ph.D. dissertation submitted by Carolyn T. MacDonald to Brown University.

Its manuscript was prepared while Julian H. Gibbs was on sabbatical leave from Brown University at the Max Planck Institute for Physical Chemistry in Göttingen, Germany, and was receiving support from the John Simon Guggenheim Memorial Foundation and from the governments of the United States and the Federal Republic of Germany under the Fulbright-Hays Act.

References

1. A. C. Pipkin and J. H. Gibbs, *Biopolymers*, **4**, 3 (1966).
2. C. T. MacDonald, J. H. Gibbs, and A. C. Pipkin, *Biopolymers*, **6**, 1 (1968).
3. C. T. MacDonald, unpublished thesis (1968).
4. H. S. Slayter, J. R. Warner, A. Rich, and C. E. Hall, *J. Mol. Biol.*, **7**, 652 (1963).
5. M. Takanami and G. Zubay, *Proc. Nat. Acad. Sci. U.S.*, **51**, 834 (1964).
6. J. R. Warner, A. Rich, and C. E. Hall, *Science*, **138**, 1399 (1962).
7. H. M. Dintzis, *Proc. Nat. Acad. Sci. U.S.*, **47**, 247 (1961).
8. H. Goldstein, D. B. Goldstein, and L. I. Lowney, *J. Mol. Biol.*, **9**, 213 (1964).
9. S. W. Englander and L. A. Page, *Biochem. Biophys. Res. Comm.*, **19**, 565 (1965).
10. M. A. Naughton and H. M. Dintzis, *Proc. Nat. Acad. Sci. U.S.*, **48**, 1822 (1962).
11. H. M. Dintzis and P. M. Knopf, *Informational Macromolecules*, H. J. Vogel et al., Eds., Academic Press, New York, 1963, p. 376.
12. R. M. Winslow and V. M. Ingram, *J. Biol. Chem.*, **241**, 1144 (1966).
13. A. R. Williamson and R. Schweet, *Nature*, **202**, 45 (1964).
14. A. R. Williamson and R. Schweet, *J. Mol. Biol.*, **11**, 358 (1965).

Received July 24, 1968

Revised November 8, 1968